Kinetics and Catalysis, Vol. 41, No. 6, 2000, pp. 826–834. Translated from Kinetika i Kataliz, Vol. 41, No. 6, 2000, pp. 907–915.

Porous Al_2O_3/Al Metal Ceramics Prepared by the Oxidation of Aluminum Powder under Hydrothermal Conditions Followed by Thermal Dehydration: I. Composition and Macrocharacteristics of Composites

S. F. Tikhov, V. B. Fenelonov, V. A. Sadykov, Yu. V. Potapova, and A. N. Salanov

Boreskov Institute of Catalysis, Siberian Division, Russian Academy of Sciences, Novosibirsk, 630090 Russia

Received July 26, 1999

Abstract—The macrotexture and mechanical properties of porous Al_2O_3/Al metal ceramics prepared by the hydrothermal treatment of aluminum powder in a closed space are studied using gravimetry, pycnometry, mercury porosimetry, and scanning electron microscopy. Analytical expressions that relate the porosity, density, and mechanical strength of parent materials and final products to the composite synthesis conditions are derived.

INTRODUCTION

The production of porous Al_2O_3/Al metal ceramics by the hydrothermal oxidation of aluminum powder in the closed space of a die mold placed in an autoclave was described in [1–4]. Then, boehmite formed on the surface of aluminum particles decomposed at 520°C. This method makes it possible to prepare strong porous composite pieces of a given shape that contain aluminum metal particles uniformly distributed in a highly porous alumina matrix. These composites are promising materials for the manufacturing of supports, catalysts, and adsorbents [2–4]. Compared to commonly used supports and catalysts based on alumina, the above composite materials exhibit higher mechanical strength and thermal conductivity.

At the same time, both the properties of these materials and methods for controlling these properties are poorly studied. Data have been published on the structure of a surface film formed in the oxidation of aluminum powder with water in a free volume at temperatures lower than 100°C [5] and on the properties of powdered products of the oxidation of aluminum alloys with water (aluminum hydroxides and, after thermal decomposition, aluminum oxides formed at high aluminum conversions) [6]. Detailed theoretical and experimental studies of the relationship between the texture of metal-ceramic materials (cermets) prepared by hydrothermal oxidation in a closed space and the composition (the conversion of aluminum) were not performed.

It is well known that a change in the solid-phase volume plays a considerable role in the formation of the porous structure of solids. The Pilling–Bedworth criterion (Δ) defined as the ratio between the volumes of final and initial phases is an important characteristic of these changes [7–10]. For a topochemical process like

$$a\mathrm{A}_{\mathrm{solid}} \longrightarrow \mathrm{B}_{\mathrm{solid}} + c\mathrm{C}_{\mathrm{gas}}$$

and the complete conversion, the Δ value can be determined by the expression

$$\Delta = V_\mathrm{B}/V_\mathrm{A} = M_\mathrm{B}\rho_\mathrm{A}/aM_\mathrm{A}\rho_\mathrm{B}, \qquad (1)$$

where V, M, and ρ are the volume, molecular weight, and true pycnometric density of the phases, respectively, and a is the stoichiometric coefficient in Eq. (1). At $\Delta > 1.0$ or $\Delta < 1.0$, the solid-phase volume increases or decreases, respectively.

Earlier, the formation of porous structures was studied in solid-phase transformations accompanied by a decrease in the volume of solids, that is, at $\Delta < 1.0$ (for example, the formation of porous carbon materials or MgO in the decomposition of Teflon or $MgCO_3$, respectively [8–10]). The process of formation of mechanically strong porous Al_2O_3/Al metal ceramics from powdered aluminum is more complicated. It was found [2, 3] that this process involves the following two key stages:

(1) The hydrothermal oxidation stage in the course of which boehmite is formed

$$\mathrm{Al}^0 + \mathrm{H_2O(O_2)} \longrightarrow \mathrm{AlOOH} + \mathrm{H_2}$$
$$(\Delta_1 = M_\mathrm{AlOOH}\rho_\mathrm{Al}/M_\mathrm{Al}\rho_\mathrm{AlOOH} = 2.00); \qquad \text{(I)}$$

(2) The stage of boehmite thermal decomposition to form Al_2O_3 with a spinel structure

$$\mathrm{AlOOH} \longrightarrow \mathrm{Al_2O_3} + \mathrm{H_2O}$$
$$(\Delta_2 = M_{\mathrm{Al_2O_3}}\rho_\mathrm{AlOOH}/M_\mathrm{AlOOH}\rho_{\mathrm{Al_2O_3}} = 0.77). \qquad \text{(II)}$$

0023-1584/00/4106-0826$25.00

The overall reaction can be described as

$$2Al + 3/2O_2 = Al_2O_3 \quad (\Delta = \Delta_1\Delta_2 = 1.54). \qquad \text{(III)}$$

To calculate the values of Δ_i, the numerical values of ρ_{AlOOH} and $\rho_{Al_2O_3}$ were taken from [8].

Thus, the solid-phase volume increases at stage (I) and decreases at stage (II). Overall process (III) is accompanied by an increase in the solid-phase volume because of the addition of oxygen and an increase in the total mass of solids, although the density of aluminum oxide is higher than that of metallic aluminum [8]. We expected that both stages would affect the formation of the composite texture.

In this work, on the basis of an analysis of previously obtained data [2–4] and new experimental results, we revealed factors controlling the porous structure and mechanical properties of a highly porous Al_2O_3/Al metal ceramics.

EXPERIMENTAL

The procedure for the preparation of Al_2O_3/Al cermets involved the following stages [1–3]:

(1) The charging of a collapsible mold of stainless steel with powdered aluminum (the design of this mold provides access for steam supplied from an autoclave to the internal space of the mold);

(2) The hydrothermal treatment of the aluminum powder in an autoclave for a given time at a constant temperature and pressure of water vapor;

(3) Steam dumping from the autoclave to terminate the hydrothermal oxidation reaction followed by slow cooling of the mold in the autoclave;

(4) The removal of mechanically strong pellets of the product from the mold, drying at 120°C, and calcination at 520°C.

The methods for cermet analysis involving the determination of apparent and true densities, pore volumes, product fractions, and mechanical strength, as well as the results of cermet characterization by scanning electron microscopy, have been described elsewhere [2–4] (see also the monograph [11] for general methodology).

RESULTS AND DISCUSSION

1. Relationship between the True and Apparent Densities of Cermets

Solid-phase reaction (I) accompanied by an increase in the solid-phase volume is performed in the closed space of a mold. Therefore, the total volume of a porous pellet (V_0) upon the complete (100%) conversion remained unchanged as in the initial state (when the mold was charged with a powder). However, reaction (II) is performed after the removal of a piece from the mold and may occur without changes in the geometric volume of the piece (in this case, a pellet) or be accompanied with some shrinkage.

Let us initially consider a situation associated with reaction (I) when the pellet volume V_0 is constant and equal to the volume of a mold. The apparent cermet density (δ_α) at an incomplete conversion α is determined by the expression

$$\delta_\alpha = m_\alpha / V_0, \qquad (2)$$

where m_α is the mass of the solid at an incomplete conversion.

The relative change in the mass of the solid at complete conversion is

$$X_0 = \frac{m_B - m_A}{m_A} = \frac{m_B}{m_A} - 1 = \frac{M_B}{aM_A} - 1 = \Delta\frac{\rho_B}{\rho_A} - 1, \qquad (3)$$

where m_A is the initial mass of the substance A and m_B is the mass of substance B at the complete conversion, and the conversion is

$$\alpha = \frac{m_\alpha - m_A}{m_B - m_A}. \qquad (4)$$

At an incomplete conversion, the relative change in the mass of the solid is determined by the relation

$$\alpha X_0 = \frac{m_\alpha - m_A}{m_A} = \frac{m_\alpha}{m_A} - 1. \qquad (5)$$

Consequently,

$$m_\alpha = (\alpha X_0 + 1)m_A. \qquad (6)$$

Note that Eqs. (3)–(6) are true only for $m_B > m_A$. Substitution of Eq. (6) into Eq. (2) gives

$$\delta_\alpha = \frac{(\alpha X_0 + 1)m_A}{V_0} = (\alpha X_0 + 1)\delta_0, \qquad (7)$$

where δ_0 is the packing density of the initial aluminum powder or the apparent density of the cermet at a conversion of zero. Equation (7) describes the relationship between the packing density of the starting alumina powder, the degree of its conversion into the oxide, and the apparent density of the cermet. It can be applied to the solid-phase transformations under discussion and other solid-phase reactions in a closed space. To do this, it is only necessary to take into account relevant changes in X_0, because this parameter characterizes each individual topochemical reaction. In particular, $X_0 = 0.89$ in overall aluminum oxidation reaction (III) involving the formation of boehmite upon hydrothermal treatment and alumina after the thermal decomposition in air, whereas $X_0 = 1.22$ in reaction (I).

Table 1 summarizes the texture characteristics of cermets obtained after the thermal decomposition of boehmite, in particular, the conversion α calculated using Eq. (4), the apparent density δ_α experimentally found from the mass and geometric volume of pellets,

and the zero density δ_0 calculated by Eq. (7). It can be seen that the calculated values of δ_0 increase with α. The shrinkage of composite pellets after calcination at 520°C can reasonably explain this phenomenon.

Indeed, let us designate the volume shrinkage factor (f_v) of the pellets as the ratio between the composite pellet volume after calcination (V_f) to the volume of the mold (V_0). Hence, it follows that

$$f_v = \frac{V_f}{V_0} = \frac{\delta'_\alpha}{\delta_\alpha}, \quad (8)$$

where δ'_α is the apparent density of the cermet in the absence of shrinkage, and δ_α is the actual apparent density of the cermet. We evaluate the coefficients f_v by assuming that the zero density is constant and equal to 1.19. The calculated values of f_v are low and fall within the range of permissible variation (at $\Delta_2 = 0.77$, this range is $0.77 \le f_v \le 1.0$). Nevertheless, these values are sufficiently high for the zero density δ_0 to noticeably change at stage (II). This shrinkage is characteristic of hydroxides that produce finely divided primary oxide particles upon the formation of pellets and calcination. Therefore, the difference between the experimental zero density and the value calculated without regard for shrinkage typically increases with the oxide (hydroxide) content of the composite.

Table 1 also gives the experimentally measured pycnometric densities (ρ_α) of cermets and the densities of an Al_2O_3 phase ($\rho_{Al_2O_3}$) calculated on this basis. In these calculations, we used the equation obtained with consideration for the density balance

$$\frac{1}{\rho_\alpha} = \frac{y}{\rho_{Al_2O_3}} + \frac{1-y}{\rho_{Al}}, \quad (9)$$

where y is the mass fraction of alumina, and ρ_i are the true densities of the corresponding components of the composites; the mass balance

$$m_\alpha = m_{Al}(1 + \alpha X_0) = m_{Al}(1 - \alpha) + \alpha m_{Al}(1 + X_0), \quad (10)$$

where the terms $m_\alpha(1 - \alpha)$ and $\alpha m_{Al}(1 + X_0)$ correspond to the masses of residual aluminum and the formed oxide, respectively; and the solid-phase volume balance is

$$\frac{m_\alpha}{\rho_\alpha} = \frac{m_{Al}(1-\alpha)}{\rho_{Al}} + \frac{\alpha m_A(1 + X_0)}{\rho_{Al_2O_3}}, \quad (11)$$

where the first and second terms on the right-hand side depend on the volumes of the residual aluminum phase and the oxide phase, respectively.

The solution to this set of equations is the following relation between the composition of the composite materials (y) and the conversion of aluminum (α):

$$y = \frac{\alpha(X_0 + 1)}{\alpha X_0 + 1}, \quad \alpha = \frac{y}{1 + X_0(1-y)}, \quad (12)$$

where $(\alpha X_0 + 1) = m_\alpha/m_{Al}$ (see Eq. (6)), and $(1 + X_0) = m_{Al_2O_3}/m_{Al}$ (see Eq. (3)).

Table 1. Textural characteristics of Al_2O_3/Al cermets depending on the degree of aluminum conversion*

Sample (conditions of preparation)	α	δ_α, g/cm^3	f_v	δ_0, g/cm^3	ρ_α, g/cm^3	$\rho_{Al_2O_3}$, g/cm^3	Δ_α	V_δ, cm^3/g
Al powder loaded into the mold	0	1.19	1.00	1.19	2.76	–	–	0.48
Hydrothermal treatment product (150°C, 0.5 h, 5 atm)	0.07	1.24	1.02	1.17	2.71	2.41	2.17	0.44
Hydrothermal treatment product (150°C, 6.5 h, 5 atm)	0.12	1.29	1.02	1.16	2.64	2.27	2.17	0.40
Hydrothermal treatment product (200°C, 2 h, 20 atm)	0.12	1.34	0.91	1.21	2.79	2.92	1.80	0.40
Hydrothermal treatment product (250°C, 3.5 h, 50 atm)	0.19	1.53	0.85	1.31	2.85	3.07	1.68	0.33
Hydrothermal treatment product (250°C, 5.0 h, 50 atm)	0.22	1.50	0.95	1.26	2.86	3.08	1.68	0.34
Hydrothermal treatment product (250°C, 6.5 h, 50 atm)	0.24	1.54	0.94	1.27	3.00	3.49	1.45	0.37

* The values of α, δ_α, and ρ_α were found experimentally and the other parameters were calculated.

Since the properties of initial reactants and products are known, and with the cited analytical formulas, we can quantitatively determine various characteristics of solids by calculating either the conversion or the composition of composite materials.

The density of aluminum oxide in composites was estimated by the following equation derived from Eq. (11):

$$\rho_{Al_2O_3} = \frac{\alpha(1 + X_0)}{\frac{\alpha X_0 + 1}{\rho_\alpha} - \frac{1 - \alpha}{\rho_{Al}}}. \quad (13)$$

The values of $\rho_{Al} = 2.76$ g/cm^3 and ρ_α were found by pycnometry; $X_0 = 0.89$; and the values of α were determined by gravimetry. Note that Eq. (13) is analogous to the simpler balance in Eq. (9). The results obtained are also presented in Table 1.

The density of alumina with a spinel structure calculated by Eqs. (13) and (9) from data on the pycnometric density of metal–oxide composites increases from 2.4 to 3.49 g/cm^3 with the time and temperature of hydrothermal oxidation and approaches a theoretical value of 3.65 g/cm^3 [12]. Note that the helium density of the starting aluminum powder is somewhat higher than the published value (2.76 and 2.69 g/cm^3, respectively). This is likely due to the formation of an oxide layer on the surface of aluminum particles during long contact with air. The helium density of a model sample of γ-Al_2O_3 (type A-1) prepared by co-precipitation was consistent with the published data (3.3 g/cm^3).

Significant deviations of the true density of various alumina oxides from the average value have been observed before [8, 12, 13]. However, the tendency towards an increase in the density of oxide with increasing intensity of the hydrothermal treatment of the resulting hydroxide is observed for the first time. A lower density can be explained by high concentrations of point and prolonged defects in the products of the gas–solid reaction. These defects appear as cationic and anionic vacancies, dislocations, coherent and incoherent boundaries between intergrowing particles and blocks different from a spinel lattice of the γ-Al_2O_3 type in density. This is typical of amorphous products of hydrothermal oxidation at the initial stages of the process. As the reaction occurs, the parallel process of product recrystallization starts to contribute to the formation of thermodynamically more stable species. It is not accidental that the degree of crystallinity of the oxide (and hence the hydroxide) considerably increases with increasing intensity of the hydrothermal treatment according to the data of electron microscopy (see the subsequent article in this issue). The existence of closed pores cannot also be excluded [12]. The density of oxide prepared at elevated temperatures and prolonged synthesis times was higher than that reported in [8]. This can be a consequence of a high degree of crystallinity and a decreased concentration of OH groups in the resulting oxide as was observed earlier in boehmite decomposition products [12].

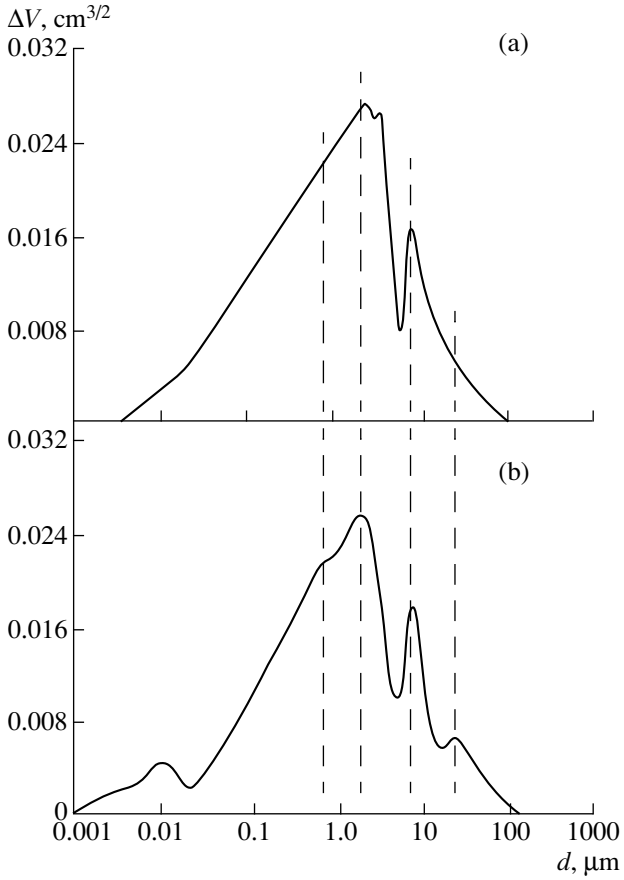

Fig. 1. Pore-size distribution in cermet composites prepared by the calcination of samples synthesized by hydrothermal treatment under the following conditions: (a) T = 150°C, $P \approx 0.5$ MPa, and $\tau = 0.5$ h. (b) T = 250°C, $P \approx 5$MPa, $\tau = 6.5$ h. The logarithmic scale is used along the x-axis; ΔV is an increase in the pore volume.

Differences in the density of aluminum oxide will also result in different changes in the volume of solids; this is represented in the general form by the Pilling–Bedworth criterion. Therefore, the values of Δ_α are presented in Table 1 with consideration for the density of alumina, which was estimated from data on the true density and composition of corresponding cermets.

Thus, the initial state of a powdered product charged into a mold significantly affects both the properties of resulting composites and changes in the properties of the product (the density) in the course of the process that occurs in parallel to the main gas–solid reaction.

2. Relationship between the Pore Volume of Al_2O_3/Al Cermets and the Degree of Aluminum Conversion

The apparent density of Al_2O_3/Al cermets, in view of a shrinkage at the stage of boehmite thermal decomposition, is described by the equation

$$\delta_\alpha = \frac{m_\alpha}{V_0 f_v} = \frac{\delta_0(\alpha X_0 + 1)}{f_v} \quad (14)$$

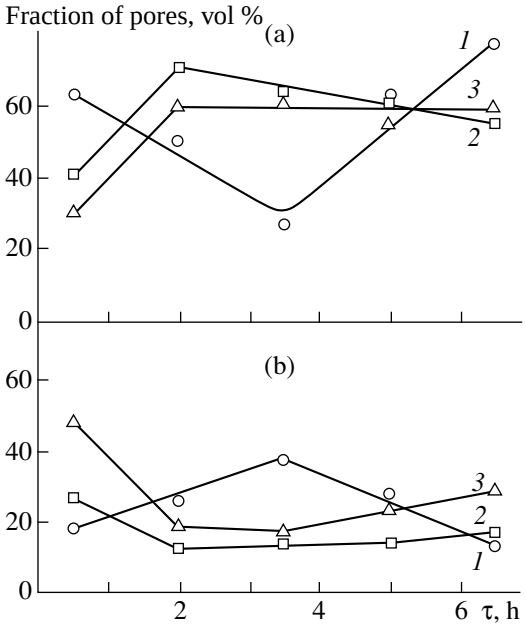

Fig. 2. Fractions of pores with diameters (a) 1–8 and (b) 10–30 μm in cermet composites as functions of time of the hydrothermal treatment at temperatures of (*1*) 150, (*2*) 200, (*3*) and 250°C.

(see Eqs. (7) and (9)).

The total volume of pores (interparticle void spaces) in a cermet prepared at the conversion α is determined by the expression

$$V = V_0 f_v - V_\alpha = V_0 f_v - \frac{m_\alpha}{\rho_\alpha}. \quad (15)$$

The specific pore volume in the cermet is equal to

$$V_\delta = \frac{V}{m_\alpha} = \frac{V_0 f_v}{m_\alpha} - \frac{1}{\rho_\alpha} = \frac{1}{\delta_\alpha} - \frac{1}{\rho_\alpha}, \quad (16)$$

where δ_0 is determined by Eq. (14), and ρ_α by Eq. (11) with substitution of Eq. (5).

Table 1 summarizes the values of V_δ calculated by Eq. (16). These values are much higher (by a factor of 3 to 4) than the experimental data obtained by mercury porosimetry. This discrepancy can be explained by the existence of mesopores and micropores with an effective pore size lower than 0.004 μm, which are inaccessible to mercury, and ultramacropores larger than 30 μm in size, which are spontaneously filled with mercury at a minimum mercury pressure. We evaluated the volume of micropores and mesopores formed in the thermal decomposition of stoichiometric boehmite on the basis of pycnometry data and an analysis of nitrogen adsorption isotherms (see the subsequent article for details). This volume does not exceed 0.044 cm^3/g (of composite). Thus, the discrepancy between the theoretical estimates (0.37–0.40 cm^3/g) and the experimental data on the pore volume obtained by mercury porosimetry (0.2–0.1 cm^3/g) [3] cannot be explained by the existence of micropores and mesopores only. This fact is indicative of the presence of extremely wide ultramacropores, which are typical of honeycomb materials, in Al_2O_3/Al cermets.

Using Eqs. (14), (9), and (12), we can obtain the following expression that relates the specific pore volume to the conversion and the packing density of the starting aluminum powder in a mold:

$$V_\delta = \frac{f_v}{\delta_0(\alpha X_0 + 1)} - \frac{1-\alpha}{\rho_{Al}(\alpha X_0 + 1)} - \frac{\alpha(X_0 + 1)}{\rho_{Al_2O_3}(\alpha X_0 + 1)}. \quad (17)$$

Based on Eq. (17), the total pore volume in a metal–oxide composite can be purposely controlled by varying the above parameters in the course of synthesis and by affecting the density of the product (aluminum oxide) through changes in the temperature and duration of the synthesis.

3. Macropore Distribution in Al_2O_3/Al Cermets

Figure 1 demonstrates two examples of the pore-size distribution as found by mercury porosimetry, and Fig. 2 shows the fractions of pores with diameters 1–8 and 10–30 μm plotted against time of the hydrothermal treatment at different temperatures on the basis of these data. The mercury pore-size measurements were performed using a particle-size fraction of 5–8 mm. Pores with an apparent size up to 50 μm were reliably determined by this method. Figure 1 indicates that the pore-size distribution for pores more than 0.1 μm in diameter remains almost unchanged even at a maximum difference in the conversion (Al_2O_3 content). The curves exhibit more or less pronounced peaks, which correspond to diameters of 32, ~10, ~3.2, and ~1 μm. This allowed us to conclude that the above distribution primarily depends on the packing characteristics and particle size of the parent aluminum powder. The average size of macropores can be estimated by the equation [11]

$$\bar{d} = 0.6D\frac{\varepsilon}{1-\varepsilon}, \quad (18)$$

where D is the average particle size of the starting powdered aluminum according to the data of dispersion analysis performed by the Coulter coulometric method, and ε is defined by the equation [10]

$$\varepsilon = \frac{\delta_\alpha V_{pore}}{1 + \delta_\alpha V_{pore}}, \quad (19)$$

where V_{pore} is the pore volume according to mercury porosimetry data. The value of $\bar{d}$ found by Eq. (18) was equal to ~2.4 μm. Pores of this size prevail in the metal–oxide composite (Fig. 1). Consequently,

macroporosity depends on the particle size of parent aluminum.

The existence of ultramacropores of size >10 μm in the sample has engaged our attention. Note that the detection of these pores by mercury porosimetry is not associated with possible aluminum amalgamation by the interaction with mercury because in this case the experimental pore volume would be higher than that calculated from the apparent and true densities. However, according to the data of mercury porosimetry, the volume of these pores in the starting aluminum powder with minimal oxide film thickness was 25–30% lower than that estimated by Eq. (16). The existence of pores of size >10 μm was also confirmed by the data of scanning electron microscopy [2]. Evidently, the fact that the gravity loading of the starting aluminum powder into a mold with tapping does not result in the closest packing plays an important role in the formation of ultramacropores. Indeed, additional pressing of the aluminum powder substantially increases the apparent density of powdered aluminum pellets and decreases their porosity (Table 2).

The indirect evidence for the existence of large ultramacropores is that a portion of mercury was spontaneously ejected from the penetrometer (a glass ampule with a calibrated capillary in which the sample was placed) as the pressure was decreased in experiments performed by mercury porosimetry. This effect, which manifested itself in the study of all samples of the given composites, was observed for the first time. Usually, after completing the measurements and fully reducing the pressure, a significant portion of mercury remained in the sample within the pellet. The above phenomenon can be explained by the existence of extremely large pores which were filled with mercury under gravity even at the stage of preliminary filling (before applying pressure) of the penetrometer. This leads to an underestimation of pore volumes. Mercury was retained by capillary forces in ordinary highly porous solids after completion of experiments, whereas in the case under discussion a portion of mercury poured out because of an extremely large pore size. Consequently, we believe that the cermet composites may be similar to porous powdered materials in the macropore structure [14].

Figure 2 indicates that the dynamics of changes in the macropore (1–8 μm) and ultramacropore (10–30 μm) fractions depending on the synthesis time was different for samples prepared at different temperatures. Taking into account data [2] obtained by scanning electron microscopy, we can conclude that two processes are responsible for the macropore distribution. One of them involves reasonably rapid complete oxidation and hydration of small aluminum particles, which exhibit higher reactivity [15], and dissolution (recrystallization) of these particles with mass transfer to coarser particles of aluminum or to interparticle boundaries. In this case, the fraction of macropores decreases, and the contribution of ultramacropores increases (Fig. 2a). The second process is associated with a slow growth of oxide (hydroxide) particles on the surface of coarse aluminum particles as they are oxidized. This results in the filling of voids and an increase in the fraction of macropores (Fig. 2b).

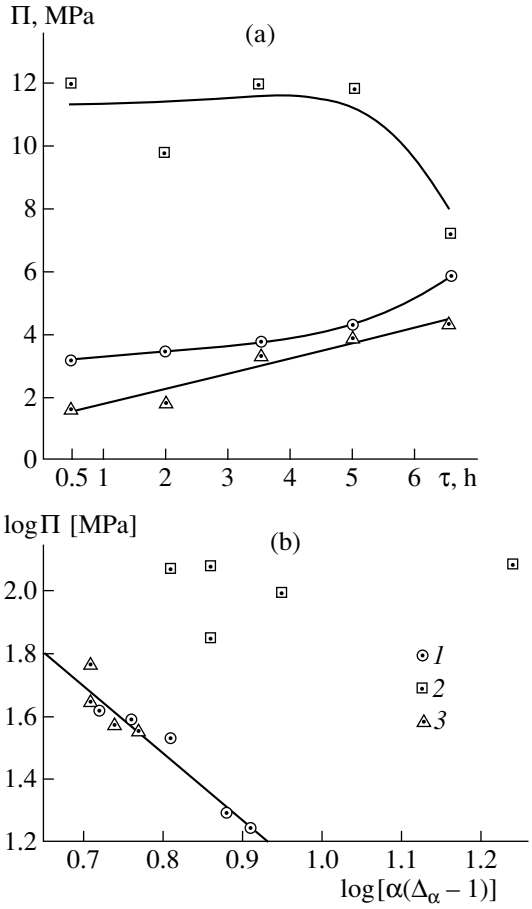

Fig. 3. Mechanical strength of composite pellets as a function of (a) time of the hydrothermal synthesis or (b) the averaged Pilling–Bedworth value. Hydrothermal treatment conditions: (*1*) T = 150°C, $P \approx 0.5$ MPa; (*2*) T = 200°C, $P \approx 2.0$ MPa; and (*3*) T = 250°C, $P \approx 5$ MPa.

Table 2. Characteristics of powdered alumina as functions of pressure

Pressure, MPa	Apparent density (δ), g/cm^3	Free volume fraction (ε_0)
0	~1.2	0.53
1	1.9	0.30
3	2.0	0.28
5	2.3	0.17

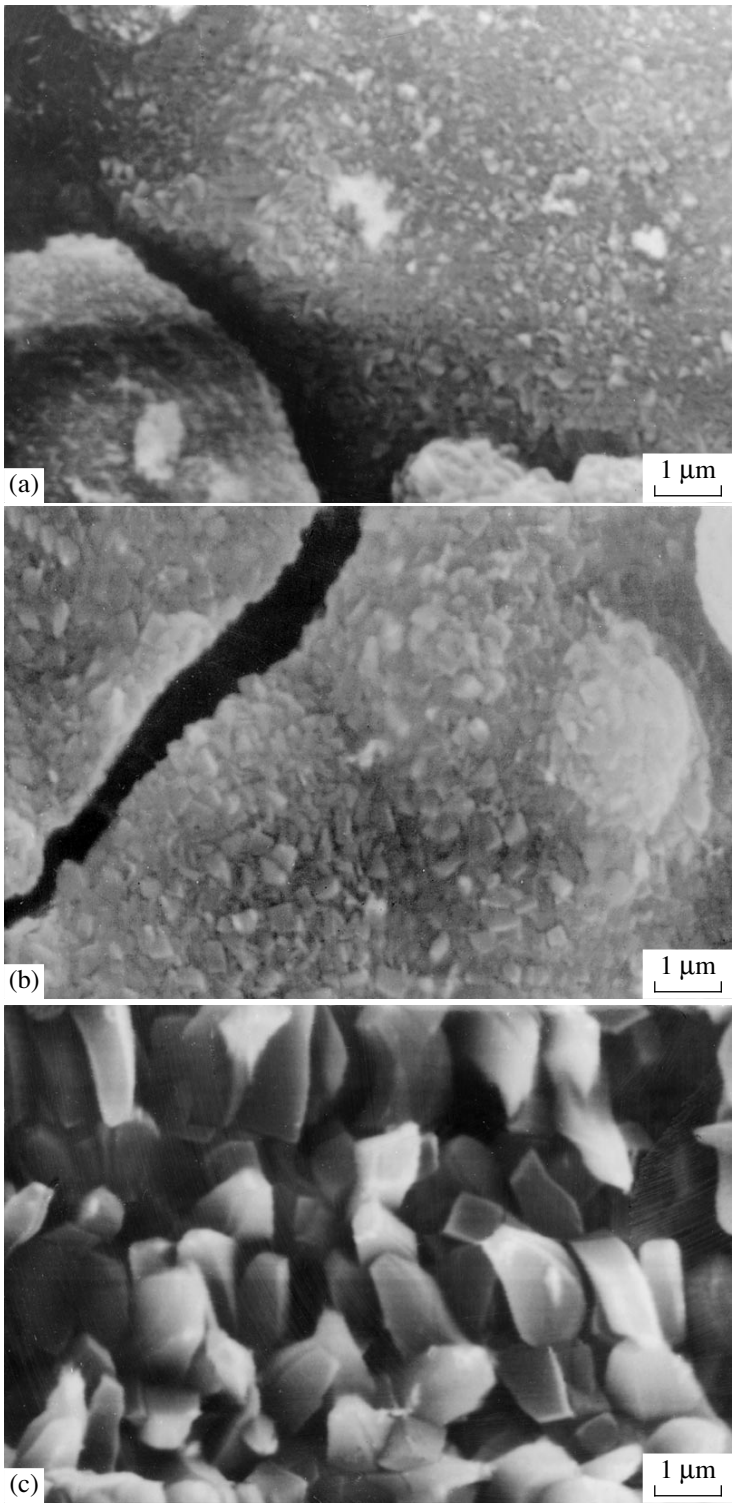

Fig. 4. Electron microscopic patterns of Al_2O_3/Al composites prepared by hydrothermal treatment followed by calcination in air. The conditions of hydrothermal treatment: (a) T = 150°C, τ = 2 h; (b) T = 200°C, τ = 0.5 h; and (c) T = 250°C, τ = 5 h.

We believe that the former process dominates at 150°C. At higher temperatures, the first stage of this process is much faster, and the pore-size distribution dynamics is controlled by the second stage. The approximate constancy of the total pore volume and the fraction of macropores and ultramacropores at synthesis times longer than 2 h regardless of the oxide fraction of the cermet (Table 1) can be explained, as mentioned above, by compacting the reaction product in the course of its recrystallization under exposure to steam.

4. Factors Responsible for the Mechanical Strength of Composite Pellets

A mechanically strong AlOOH/Al composite is formed in the course of hydrothermal treatment of an aluminum powder in a closed space. This composite also preserved its properties after thermal decomposition in air. As a first approximation, we believe that the main driving force for the self-consolidation of composite particles is an increase in the volume, which produces interparticle pressure within the mold because of the solid-phase reaction. When the apparent density of powdered aluminum pressed in pellets at various pressures (Table 2) is compared with the apparent density of Al_2O_3/Al cermets (Table 1), it can be concluded that the isostatic pressure produced within the mold does not exceed 1 MPa. However, in experiments with powdered alumina, we found that this pressure is sufficient for transforming the powder into a consolidated solid. Moreover, it may be expected that the composite volume and hence the consolidating pressure will be higher at the stage of hydrothermal treatment.

It is well known that the mechanical strength (Π) increases with a decrease in the porosity (ε) of the material as expressed in the general form by the following semiempirical Bal'shin equation [16]:

$$\Pi = \Pi_0(1-\varepsilon)^m. \quad (20)$$

In Eq. (20), the porosity ε of solids prepared by thermal decomposition of any substances with the conversion α is determined as follows [9]:

$$\varepsilon = \alpha(1-\Delta), \quad (21)$$

where $\Delta < 1$.

However, a reverse process of filling the space between pores formed by aluminum particles takes place in the synthesis of alumina cermets. The increase (ξ) in the solid volume at $\Delta > 1$ can be expressed by the equation

$$\xi = \alpha(\Delta-1). \quad (22)$$

On this basis, we expect that the strength of composite pellets is proportional to an increase in the volume of solids in a fixed volume of the mold

$$\Pi = \Pi_0\xi^m = \Pi_0[\alpha(\Delta-1)]^m. \quad (23)$$

Figure 3a presents the experimental data on the mechanical strength of cermet pellets prepared at various hydrothermal treatment temperatures and times. Figure 3b shows a logarithmic plot of the above values as functions of an increase in the solid volume found according to Eq. (23). The values of Δ_α from Table 1 were used in the calculations Δ. It can be seen in Fig. 3 b that for the samples synthesized at 150 and 250°C this function is linearized in the form $y = A + Bx$, where $A \approx 2.2$, and $B \approx 2.17$. The value of $\Pi_0 \approx 100$ MPa calculated on the basis of A is close to a pressure that provides 30–40% shrinkage of aluminum powder upon pressing in order to produce pieces with a maximum density [17]. Cermets synthesized at 200°C are inconsistent with the general pattern, probably because of their macrotexture peculiarities. Indeed, according to the data of scanning electron microscopy, alumina particles of any type dominate the composites that follow the general pattern. Oxide sponge particles and elongated faceted alumina particles are characteristic of the cermets synthesized at 150 and 250°C, respectively (Figs. 4a and 4b). Oxide particles of both of these types were present in the cermet synthesized at 200°C (Fig. 4c). It is well known that the structure of aluminum oxide significantly affects the mechanical properties of sintered aluminum powders [17]. Thus, an important factor responsible for the mechanical strength of pellets is the shearing resistance of particles relative to each other. Cermets prepared at 200°C exhibit maximum shearing resistance because of pinion effects (see Fig. 4). A similar anomaly in the dependence of the mechanical strength of γ-Al_2O_3 pellets on the temperature of hydrothermal treatment accompanied by the formation of boehmite was observed earlier [18].

CONCLUSION

We derived analytic expressions that relate macroproperties, such as the bulk density and pore volume of Al_2O_3/Al composites and the packing density of the parent material to the composition (the degree of aluminum conversion) and density of the product (the Pilling–Bedworth value). We found that the pore-size distribution in the composite formed depends on the particle-size distribution of parent aluminum at low temperatures and short times of the synthesis. At long times of synthesis, the aggregates of coarse alumina particles come into play, taking a considerable part in the distribution of macropores. Based on an empirical equation that relates the mechanical strength to the pore volume and the Pilling–Bedworth value, we suggested the physicochemical characteristics of mechanical contacts between composite macroparticles.

ACKNOWLEDGMENTS

This work was supported by the Russian Foundation for Basic Research (project no. 99-03-32853).

REFERENCES

1. Azarov, S.M., Romanenkov, V.E., and Smirnova, T.A., *Poroshk. Metallurg.*, 1988, no. 12, p. 62.
2. Tikhov, S.F., Salanov, A.N., Palesskaya, Yu.V., *et al.*, *React. Kinet. Catal. Lett.*, 1998, vol. 64, no. 2, p. 301.
3. Tikhov, S.F., Sadykov, V.A., Potapova, Yu.V., *et al., Stud. Surf. Sci. Catal.*, 1998, vol. 118, p. 797.
4. Tikhov, S.F., Sadyfov, V.A., Potapova, Yu.V., *et al.*, *Rec. Adv. Catal. Mater.*, Boston, 1998, vol. 497, p. 121.
5. Zhilinskii, V.V., Lokenbakh, A.K., and Lepin', L.K., *Izv. Akad. Nauk Latv.SSR*, 1986, no. 2, p. 151.

6. Yakerson, V.I., Dykh, Zh.L., Subbotin, A.N., *et al.*, *Kinet. Katal.*, 1995, vol. 36, no. 6, p. 918.
7. Pliiling, N.B. and Bedworth, R.E., *J. Inst. Met.*, 1923, no. 1, p. 529.
8. Fenelonov, V.B., *Kinet. Katal.*, 1994, vol. 35, no. 5, p. 795.
9. Fenelonov, V.B., *React. Kinet. Catal. Lett.*, 1994, vol. 52, no. 2, p. 367.
10. Fenelonov, V.B., *Doctoral (Chem.) Dissertation*, Novosibirsk: Inst. of Catalysis, 1987.
11. Webb, P.A. and Orr, C., *Analytical Methods in Fine Particle Technology*, Norcross: Micromeritics., 1997, p. 193.
12. Wilson, A.J. and Stacey, M.H., *J. Colloid Interface Sci.*, 1981, vol. 82, no. 2, p. 507.
13. Wefers, K., *Alumina Chemicals: Science and Technology Handbook*, Hart, L.D., Ed., Westerwille: A.C.S. Inc., 1990, p. 13.
14. Leonov, A.N., Smorygo, O.L., Romashko, A.N., *et al.*, *Kinet. Katal.*, 1998, vol. 39, no. 6, p. 691.
15. Lur'e, B.A., Chernyshev, A.N., Perova, N.N., and Svetlov, B.S., *Kinet. Katal.*, 1976, vol. 17, no. 6, p. 1453.
16. Bal'shin, M.Yu., *Nauchnye osnovy poroshkovoi metallurgii i metallurgii volokna* (Scientific Foundation of Powder Metallurgy and Filament Metallurgy), Moscow: Metallurgiya, 1972.
17. Gopienko, V.G., Smagorinskii, M.E., Grigor'ev, A.A., and Bellavin, A.D., *Spechenye materialy iz aluminievykh poroshkov* (Sintered Materials from Aluminum Powder), Moscow: Metallurgiya, 1993.
18. Chertov, V.M., Tsyrina, V.V., and Kaganovskaya, V.A., *Zh. Prikl. Khim.*, 1992, no. 11, p. 2585.